separations

MDPI

Article

Separation and Recovery of Fe and REEs from a Hydrochloric Acid Leachate of NdFeB Waste Using Aliquat 336-Based Solvent Extraction

Lushuai Yao [1], Zishuai Liu [1,2,3,*], Zhihui Zhao [1], Qianwen Li [1], Enhao Li [1] and Huiyang Lin [1]

[1] Jiangxi Provincial Key Laboratory of Low-Carbon Processing and Utilization of Strategic Metal Mineral Resources, Jiangxi University of Science and Technology, Ganzhou 341000, China; yhaf799196919@163.com (L.Y.); zhaozhihui1998@163.com (Z.Z.); 18379934036@163.com (Q.L.); lehleh123456@163.com (E.L.); 18779748440@163.com (H.L.)
[2] Key Laboratory for Ferrous Metallurgy and Resources Utilization of Ministry of Education, Wuhan University of Science and Technology, Wuhan 430081, China
[3] Hubei Provincial Key Laboratory for New Processes of Iron Making and Steel Making, Wuhan University of Science and Technology, Wuhan 430081, China
* Correspondence: liuzishuai87@126.com

Abstract

Neodymium–iron–boron (NdFeB) waste represents a valuable secondary source of rare earth elements (REEs). However, existing recovery technologies face several challenges, such as the difficulty of selectively recovering REEs, the generation of large volumes of secondary iron-rich slag, and an overall low level of comprehensive resource utilization. In this study, Aliquat 336 was applied for the selective extraction and separation of REEs and iron (Fe) from hydrochloric acid leachate derived from NdFeB waste. Experimental results showed that under optimized conditions—specifically, a 15% Aliquat 336 concentration, an organic-to-aqueous phase ratio of 1:2, and a 2 min extraction time—Fe extraction efficiency reached 99.93% after three-stage countercurrent extraction, while REEs were predominantly retained in the aqueous phase. Subsequent oxalic acid precipitation of the raffinate yielded $RE_2(C_2O_4)_3{\cdot}10H_2O$ with a purity of 99.60%. Moreover, under stripping conditions of 2 mol/L NaOH, a phase ratio of 2:1 (aqueous to organic), and a 2 min contact time, over 99.21% of Fe was stripped after three-stage countercurrent stripping, resulting in $Fe(OH)_3$ with a purity of 99.26%. The extraction mechanism followed an anion-exchange process: under high chloride ion concentrations, Fe^{3+} formed anionic $FeCl_4^-$ complexes, which were exchanged with Cl^- ions in Aliquat 336 and transferred into the organic phase, whereas RE^{3+} cations remained in the aqueous phase, enabling efficient separation of Fe and REEs. These findings provide important insights for improving the comprehensive utilization of NdFeB waste and promoting the green and sustainable development of secondary rare earth resource recycling.

Keywords: NdFeB waste; leachate; solvent extraction; rare earth; iron; separation; Aliquat 336

Academic Editor: Guoquan Zhang

Received: 28 January 2026
Revised: 11 February 2026
Accepted: 13 February 2026
Published: 16 February 2026

1. Introduction

Neodymium–iron–boron (NdFeB) magnets dominate the global market due to their exceptional magnetic properties, accounting for over 90% of worldwide high-performance magnet production [1]. However, the short lifecycle of NdFeB-based products leads to substantial waste generation, with approximately 60–73% of industrial scrap originating

from manufacturing processes [2]. The recovery of rare earth elements (REEs) and iron (Fe) from NdFeB waste is of significant importance, as these materials contain about 30 wt.% REEs—higher than the concentrations found in primary ores—and approximately 70 wt.% Fe. This dual-value composition not only mitigates supply risks associated with critical raw materials but also supports the sustainable management of industrial byproducts [3,4].

The oxidation roasting–hydrochloric acid leaching process is the most widely used method for recovering rare earth elements (REEs) from NdFeB waste [5,6]. This approach involves roasting NdFeB waste at temperatures between 700 and 800 °C to oxidize the material, yielding a calcined product [7]. Subsequently, the calcined product is leached with hydrochloric acid, enabling nearly complete dissolution of rare earth oxides, whereas iron oxide remains only partially dissolved. The resulting hydrochloric acid leachate exhibits a complex composition, primarily containing REEs, Fe, and minor amounts of aluminum impurities [8]. Typically, after impurity removal, REEs are separated and recovered via solvent extraction using cationic extractants such as 2-ethylhexyl phosphonic acid mono-2-ethylhexyl ester (P507), which selectively extract REE^{3+} ions, while iron largely remains in the aqueous phase due to its low extractability [9–11]. The purified REE solution is then subjected to chemical precipitation followed by calcination to produce rare earth oxides. In conventional recycling processes, iron is treated as an impurity and removed through neutralization. Although this approach is well established, it results in the loss of highly concentrated iron species, leading to low comprehensive resource utilization efficiency of secondary rare earth resources. Therefore, it is essential to develop a novel method that is capable of simultaneously achieving efficient recovery of rare earth elements and effective iron recovery, thereby enhancing the overall utilization of secondary rare earth resources.

Aliquat 336, a quaternary ammonium salt, is widely recognized for its effectiveness in solvent extraction, particularly in the separation of anionic species [12–14]. It has been successfully applied to recover metal ions such as vanadium, molybdenum, and zinc from complex aqueous solutions [15–17]. Notably, Aliquat 336 maintains high extraction efficiency and selectivity under strongly acidic conditions ($pH \leq 1$), without requiring prior adjustment of solution composition. The extraction mechanism is primarily based on anion exchange. In hydrochloric acid solution, rare earth ions exist as cations (REE^{3+}) and do not form chloride complexes, whereas iron forms the anionic $FeCl_4^-$ complex in high-concentration HCl media [18,19]. This distinct difference in speciation enables Aliquat 336 to selectively extract $FeCl_4^-$ over REE^{3+}, making it a promising candidate for separating iron from REEs in hydrochloric acid leachate. However, despite its potential, the application of Aliquat 336 for the simultaneous recovery of Fe and REEs from NdFeB waste has not been extensively explored.

This study aims to develop a novel process for the separation and recovery of Fe and REEs from hydrochloric acid leachate of NdFeB waste (HLNW) using Aliquat 336-based solvent extraction. This research focuses on optimizing extraction conditions and elucidating both the extraction and stripping mechanisms. The findings are expected to provide valuable insights into the sustainable recovery of Fe and REEs from NdFeB waste, thereby contributing to the advancement of resource recycling technologies.

2. Experimental Section

2.1. Materials and Reagents

The NdFeB waste was obtained from a Ganzhou Rare Earth Waste Recycling Company. Prior to leaching, the material was subjected to oxidative calcination at 700 °C, followed by hydrochloric acid leaching. Based on our previous study [20], the optimal leaching conditions for the calcined NdFeB waste were established as follows: 4 mol/L hydrochloric

acid concentration, a liquid-to-solid ratio of 5:1 (v/m), a leaching temperature of 90 °C, and a duration of 60 min. After completion of the leaching process, solid–liquid separation was performed to obtain the hydrochloric acid leachate of NdFeB waste (HLNW). The main chemical composition of the HLNW is summarized in Table 1.

Table 1. The primary chemical constituents of HLNW(g/L).

Item	Nd	Ce	Gd	Pr	Fe	Al	Ca	Si	pH *
Con.	14.41	2.10	6.78	7.77	7.59	1.23	0.006	0.01	−0.3

* Note: pH is a dimensionless quantity.

Aliquat 336 (tri-n-octylmethylammonium chloride), with a purity of 99%, was purchased from Adamas Company, Shanghai, China and employed as the extractant. Sec-octanol (99% purity, Macklin Company, Shanghai, China) was used as the phase modifier, and sulfonated kerosene served as the diluent. Sodium hydroxide (NaOH) and hydrochloric acid (HCl) were employed for pH adjustment, while oxalic acid dihydrate ($H_2C_2O_4 \cdot 2H_2O$) was used as the precipitating agent. All reagents were of analytical grade.

2.2. Experimental Operations

Preparation of the organic phase: Accurately measure the predetermined volumes of Aliquat 336 (15%), sec-octanol (20%), and sulfonated kerosene (65%), transfer the mixture into a beaker equipped with a magnetic stirrer, and stir at 600 rpm for 2 h to ensure complete homogenization. The resulting homogeneous organic phase is ready for use in solvent extraction.

Extraction: Accurately measure a volume of 100 mL of HLNW, add the organic phase, and transfer the mixture into a beaker equipped with a magnetic stirrer. Stir the mixture at 600 rpm and room temperature for a specified duration. After stirring, carefully transfer the mixture into a separatory funnel and allow it to stand for a defined period to ensure complete phase separation. Subsequently, separate the aqueous and organic phases to obtain the raffinate and the loaded organic phase, respectively. The concentrations of Fe and REEs in the raffinate are then determined, and the extraction efficiencies are calculated accordingly.

REEs precipitation: Add the raffinate and solid oxalic acid to a beaker, then heat the mixture and stir at 500 r/min. The precipitation conditions of REEs are as follows: a mole ratio [$n(C_2O_4)$: n(REEs)] of 4.5, precipitation time of 30 min, and precipitation temperature of 60 °C. After the reaction is complete, separate the precipitants to obtain the rare earth oxalates and precipitated REEs solution.

Stripping: Accurately measure the loaded organic phase obtained from the counter-current extraction process, add a volume of 100 mL of NaOH solution, and transfer the mixture into a beaker equipped with a magnetic stirrer. Stir the mixture at 600 rpm and room temperature for a specified duration. After stirring, carefully transfer the mixture into a separatory funnel and allow it to stand for a defined period to ensure complete phase separation. Subsequently, separate the aqueous and organic phases to obtain the iron-rich solution and the regenerated organic phase, respectively. For the iron-rich solution, perform additional filtration to effectively separate the reddish-brown precipitate from the supernatant liquid after iron sedimentation.

Regeneration: A volume of 100 mL of the barren organic phase was mixed with hydrochloric acid, serving as the regeneration reagent, and subjected to the regeneration reaction under the specified conditions. The resulting mixture was then transferred to a pear-shaped separating funnel to allow complete phase separation. This regeneration

process was repeated three times to ensure full recovery of the organic phase, yielding the regenerated organic phase at the end.

The concentrations of Fe and rare earth elements (REEs) in the iron-rich solution are then determined, and the stripping efficiencies are calculated accordingly. Without considering volume changes during the experiments, the extraction efficiency (E_1), stripping efficiency (E_2), distribution ratios (D), separation factor of ions a and b after extraction ($\beta_{a,b}$) and precipitation efficiency of the REEs are calculated according to Equations (1)–(5), respectively.

$$E_1 = \frac{C_0 - C_1}{C_0} \times 100\% \quad (1)$$

$$E_2 = \frac{C_2 \times (O/A)_1}{(C_0 - C_1) \times (O/A)_2} \times 100\% \quad (2)$$

$$D = \frac{(C_0 - C_1)V_1}{C_1 V_2} \quad (3)$$

$$\beta_{a,b} = \frac{D_a}{D_b} \quad (4)$$

$$P = \frac{C_1 V_1 - C_3 V_3}{C_1 V_1} \times 100\% \quad (5)$$

where C_0 and C_1 denote the concentrations of ions in the HLNW and raffinate, respectively, expressed in g/L; V_1 and V_2 represent the volumes of the raffinate and loaded organic phase, respectively, in mL; C_2 refers to the concentration of the metal in the stripped iron-rich solution, expressed in g/L; and $(O/A)_1$ and $(O/A)_2$ are the phase ratios for extraction and stripping, respectively; C_3 (g/L) and V_3 (L) are the concentration and volume of metal ions in the precipitated REEs solution, respectively.

2.3. Analytical Methods

The concentrations of REEs in the HLNW were determined by single-channel scan inductively coupled plasma optical emission spectrometry (ICP-OES, ULTIMA 2, JOBIN YVON, Paris, France). The concentrations of other ions in the HLNW were analyzed using inductively coupled plasma optical emission spectrometry (ICP-OES, IRIS Intrepid II XDL, Thermo Electron Corporation, Sugar Land, TX, USA). Solution pH values were measured with a pH meter (PHS-3C, INESA Scientific Instrument Co., Ltd., Shanghai, China). The organic phase was characterized by Fourier transform infrared spectroscopy (FTIR, Thermo Nicolet NEXUS, Sugar Land, TX, USA), ultraviolet–visible spectrophotometry (UV-vis, UV-2700, Shimadzu, Tokyo, Japan), and time-of-flight mass spectrometry (TOF-MS, Bruker Daltonics Inc., timsTOF Flex, Bremen, Germany). Solid products were characterized by X-ray diffraction (XRD, D/MAX 2500PC, Rigaku, Tokyo, Japan) and field emission scanning electron microscopy (FE-SEM, ΣIGMA, Carl Zeiss, Jena, Germany).

3. Results and Discussion

3.1. Selective Extraction and Separation of Fe and REEs

3.1.1. Effect of Initial pH on the Extraction of Fe and REEs

The solution pH is a critical parameter in solvent extraction processes. Given that the HLNW exhibits exceptionally high acidity with a pH value of −0.3, it is essential to investigate the influence of solution pH on the extraction and separation of REEs and Fe. This study evaluates the effects of varying initial pH values on the extraction efficiency and selectivity for Fe and REEs under the following conditions: an organic-to-aqueous phase ratio (O/A) of 1:2, an Aliquat 336 concentration of 20%, a sec-octanol concentration

of 20%, an extraction temperature of 30 °C, and an extraction time of 2 min. The results are presented in Figure 1.

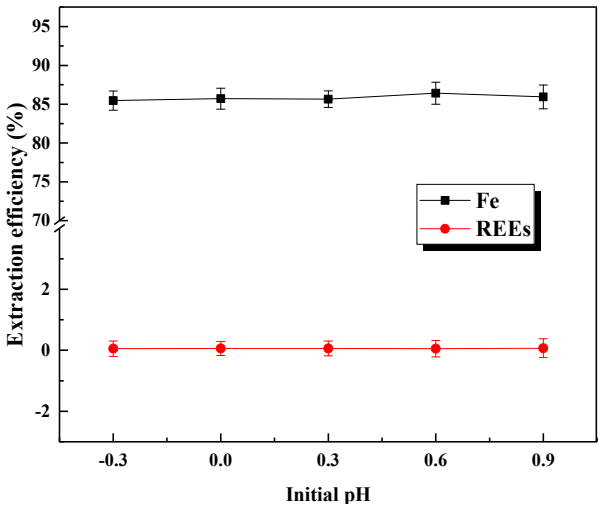

Figure 1. Effect of initial pH on the separation of Fe and REEs.

As shown in Figure 1, as the pH value increased, the extraction efficiencies of both Fe and REEs exhibited no significant variation. The extraction efficiency of Fe consistently exceeded 85%, while the co-extraction efficiency of REEs remained below 0.5%. These findings indicated that Aliquat 336 could effectively achieve efficient separation and extraction of Fe from REEs under highly acidic conditions. Therefore, the pH of the HLNW was not adjusted in subsequent experiments. The results demonstrate that Aliquat 336 enables efficient extraction under strongly acidic conditions, consistent with our previous findings on the separation of vanadium and aluminum from oxalic acid leaching solutions of vanadium-bearing shale [13,16].

3.1.2. Effect of Aliquat 336 Concentration on the Extraction of Fe and REEs

During the solvent extraction process, increasing the concentration of the extractant promoted the forward progression of the extraction reaction and enhanced the extraction efficiency. The effect of Aliquat 336 concentration on the separation of Fe and REEs was investigated under the following conditions: an organic-to-aqueous phase ratio (O/A) of 1:2, a sec-octanol concentration of 20%, an extraction temperature of 30 °C, and an extraction time of 2 min. The experimental results are presented in Figure 2.

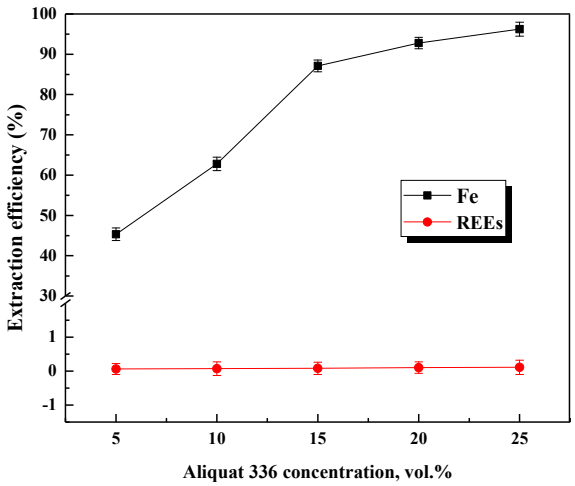

Figure 2. Effect of Aliquat 336 concentration on the separation of Fe and REEs.

As shown in Figure 2, with the concentration of Aliquat 336 increased, the extraction efficiencies of Fe progressively increased, whereas the extraction efficiencies of REEs remained unchanged and approached zero. Specifically, when the Aliquat 336 concentration was 10%, the Fe extraction efficiency was only 62.80%. Increasing the Aliquat 336 concentration to 15% resulted in a significant increase in the Fe extraction efficiency to 87.71%, with the rare earth extraction efficiency remaining as low as 0.08%. Further increasing the Aliquat 336 concentration to 20% yielded only a marginal improvement in the Fe extraction efficiency, by an additional 5.05%. Therefore, an Aliquat 336 concentration of 15% was deemed optimal for maximizing Fe extraction efficiency while minimizing REEs extraction efficiency.

Sec-octanol concentrations below 20% (v/v) consistently resulted in third-phase formation during extraction—characterized by an intermediate emulsified layer—whereas at 20% (v/v), complete and rapid phase separation was achieved: the organic and aqueous phases separated cleanly within minutes, with no observable third phase. Therefore, the sec-octanol concentration exerted no statistically significant influence on the extraction efficiencies of REEs and Fe; its primary function is confined to modulating interfacial tension and enhancing phase disengagement kinetics. Consequently, sec-octanol dosage was not treated as a key factor governing extraction efficiency and is therefore not elaborated upon.

3.1.3. Effect of Phase Ratio on the Extraction of Fe and REEs

The phase ratio (O/A) denotes the volume ratio of the organic phase to the aqueous phase. When the phase ratio (O/A) was less than 1, the extraction exhibited an enrichment effect. At an Aliquat 336 concentration of 20%, a sec-octanol concentration of 20%, an extraction temperature of 30 °C, and an extraction time of 2 min, experiments were conducted using various phase ratios, and the results are presented in Figure 3.

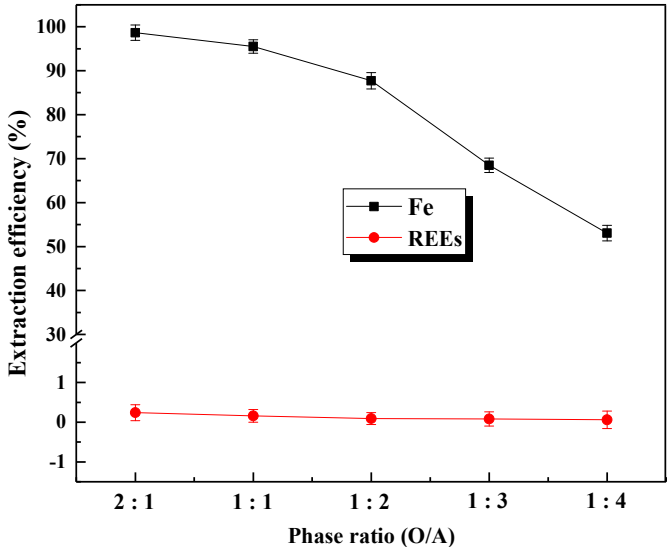

Figure 3. Effect of phase ratio on the separation of Fe and REEs.

As illustrated in Figure 3, the Fe extraction efficiencies decreased as the phase ratio diminished. When the phase ratio was 1:1, though iron extraction efficiencies exceeding 90% were achieved, effective iron enrichment could not be realized. At a phase ratio of 1:2, the Fe extraction efficiency was 87.71%, while the REEs extraction efficiencies remained as low as 0.09%. A further reduction in the phase ratio resulted in a notable decline in the Fe extraction efficiency. Consequently, a phase ratio of O/A = 1:2 was determined to be optimal.

3.1.4. Effect of Extraction Time on the Extraction of Fe and REEs

Extraction time significantly influences both extraction efficiency and kinetic behavior. Under an Aliquat 336 concentration of 20%, a sec-octanol concentration of 20%, an extraction temperature of 30 °C, and an organic-to-aqueous phase ratio (O/A) of 1:2, experiments were conducted using various extraction times, and the results are presented in Figure 4.

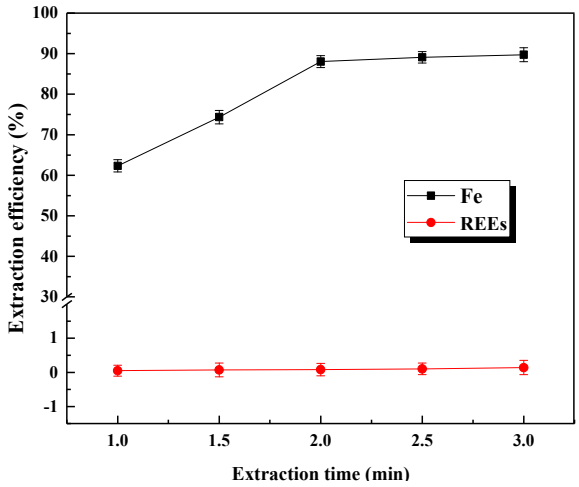

Figure 4. Effect of extraction time on the separation of Fe and REEs.

As shown in Figure 4, the iron extraction efficiency gradually increased as the extraction time increased. At 2 min, the extraction efficiency reached 88.05%; further extension yielded only a marginal increase. In contrast, the extraction of rare earth elements was not significantly affected by the extraction time and remained consistently close to zero. Therefore, an extraction time of 2 min was established as optimal. These results demonstrated that Aliquat 336 enabled efficient and rapid iron extraction, consistent with our previous findings on the separation of vanadium and aluminum from oxalic acid leaching solutions of vanadium-bearing shale [13,16].

3.1.5. Countercurrent Extraction of Fe and REEs

Based on the aforementioned optimal extraction conditions, the McCabe–Thiele plot of Fe extraction was determined. As illustrated in Figure 5, the theoretical extraction stage for Fe was two stages. To ensure complete and thorough extraction of Fe, the actual extraction stage was typically set to be one stage higher than the theoretical value. Consequently, the extraction stage for Fe was determined to be three stages.

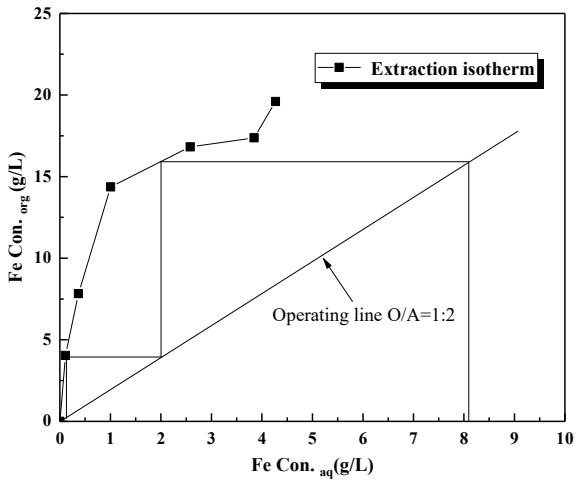

Figure 5. McCabe–Thiele plot of Fe extraction.

To evaluate the separation efficiency of Fe and REEs, countercurrent extraction experiments were conducted on the HLNW using Aliquat 336 under the following optimal conditions: 15% Aliquat 336 concentration, 20% sec-octanol concentration, a 2 min extraction time, an organic-to-aqueous phase ratio (O/A) of 1:2, and three extraction stages. The experimental results are summarized in Table 2. The data indicate that after three-stage countercurrent extraction, the extraction efficiency of Fe reached 99.92%, whereas that of REEs was only 0.18%. It is well established that a higher extraction separation factor signifies easier separation of the two ions via solvent extraction. According to Table 2, the separation factor of Fe and REEs was as high as 695,200, demonstrating that Fe and REEs can be very easily separated in the hydrochloric acid system through solvent extraction with Aliquat 336.

Table 2. Results of the three-stage countercurrent extraction.

Items	Concentration (g/L)		Extraction Efficiency (%)		Separation Factor (β)
	Fe	REEs	Fe	REEs	
HLNW	7.59	33.06			
Raffinate	0.006	33.00	99.92%	0.18%	695200
Fe-loaded organic phase	15.17	0.12			

3.1.6. Mechanism of Selective Separation of Fe and REEs

FTIR of the Loaded Organic Phase

The molecular formula of Aliquat 336 is $[(C_8H_{17})_3CH_3N]Cl$, and its structural formula is $[R_4N]\cdot Cl$. To elucidate the extraction and separation mechanisms of Fe and REEs, FTIR analyses were conducted on both pure Aliquat 336 and the Fe-loaded organic phase, respectively. The results are presented in Figure 6 and Table 3.

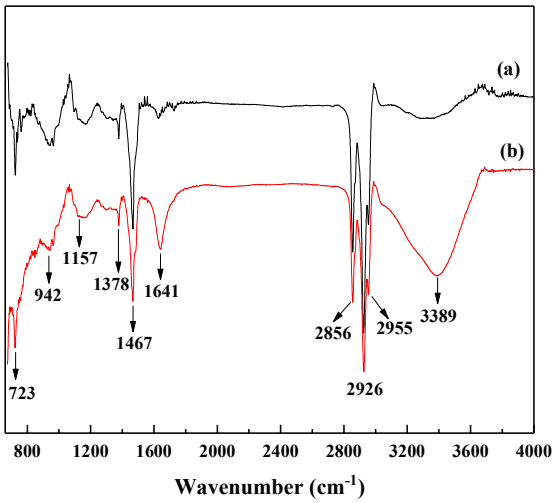

Figure 6. FTIR spectra of the organic phase. (**a**) pure Aliquat 336. (**b**) Fe-loaded organic phase.

Table 3. Assignment of the vibrations in the FTIR spectra of the organic phase presented in Figure 6.

Wavenumber (cm^{-1})	Assignment	References
3389, 1641	O-H	[21]
2955, 2926, 2856, 1378	CH_3—, —CH_2—	[22]
1467	R_4N—	[23]
1157	$\upsilon_{C\text{-}N}$	[23]
723	γ-$(CH_2)_n$-, n ≥ 4	[22]

The results presented in Figure 5 and Table 3 indicate that, for the pure Aliquat 336, the peak at 3389 cm^{-1} corresponded to the O-H stretching vibration, while the peak at 1641 cm^{-1} was attributed to the bending vibration of H_2O [21]. The characteristic peaks at 2955 cm^{-1}, 2926 cm^{-1}, 2856 cm^{-1}, and 1378 cm^{-1} were attributed to the C—H stretching vibrations of methyl and methylene groups [22], whereas the absorption band at 1467 cm^{-1} corresponds specifically to the vibrational mode of the quaternary ammonium cation (R_4N^+) [23], serving as a distinctive signature for its presence. For the Fe-loaded organic phase, no significant shifts or new/missing characteristic peaks were observed in the infrared spectrum; only variations in peak intensity were detected. This indicates that infrared spectroscopy has limited sensitivity in identifying differences in the chemical environments of functional groups between the two organic phases.

UV-Vis of the Loaded Organic Phase

FTIR requires the energy of electromagnetic waves to match specific molecular vibrational energy levels, enabling the detection of subtle structural differences in the organic phase. However, in this study, infrared spectroscopy failed to detect the state of iron in the Fe-loaded organic phase. This may be attributed to the absorption wavelength of Fe-containing functional groups being outside the detection range of infrared spectroscopy. Consequently, UV-vis spectrophotometry was employed to analyze the Fe-loaded organic phase and identify the functional groups associated with the anions. The results are presented in Figure 7.

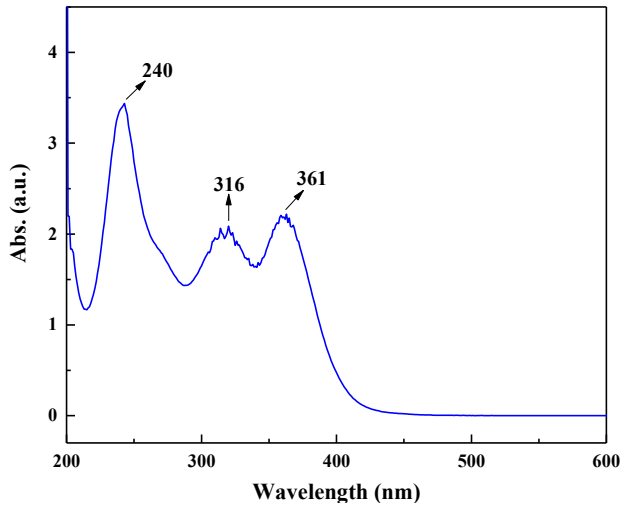

Figure 7. UV-vis of the loaded organic phase.

As shown in Figure 6, distinct characteristic peaks were observed at 240 nm, 316 nm, and 361 nm. According to reference [24], these peaks were attributed to $FeCl_4^-$ ions. Therefore, it could be concluded that Fe in the Fe-loaded organic phase existed in the form of $FeCl_4^-$ anions, with the structural formula of the extracted complex being $R_4N{\cdot}FeCl_4$. $R_4N{\cdot}FeCl_4$ represents a class of quaternary ammonium tetrachloroferrate(III) salts, in which the R_4N^+ cation is paired with the tetrahedral $FeCl_4^-$ anion (tetrachloroferrate), forming organic–inorganic hybrid materials with applications in magnetism, electronics, and catalysis. These compounds exhibit intriguing physical properties, such as phase transitions, ferroelectricity, and magnetic ordering, which are highly dependent on the nature of the organic R groups. Based on these findings, it is reasonable to infer that the extraction mechanism of iron by Aliquat 336 followed an anion exchange mechanism.

TOF-MS of the Loaded Organic Phase

To further verify that the Fe-loaded organic phase formed the extracted complex $R_4N{\cdot}FeCl_4$, the TOF-MS analysis was conducted on the loaded organic phase. The results, presented in Figure 8, show a distinct peak at m/z 567.36 in the positive ion mode. Given that the theoretical molecular weight of $R_4N{\cdot}FeCl_4$ is 566.36, this peak strongly indicates that $R_4N{\cdot}FeCl_4$ molecules were present in the Fe-loaded organic phase.

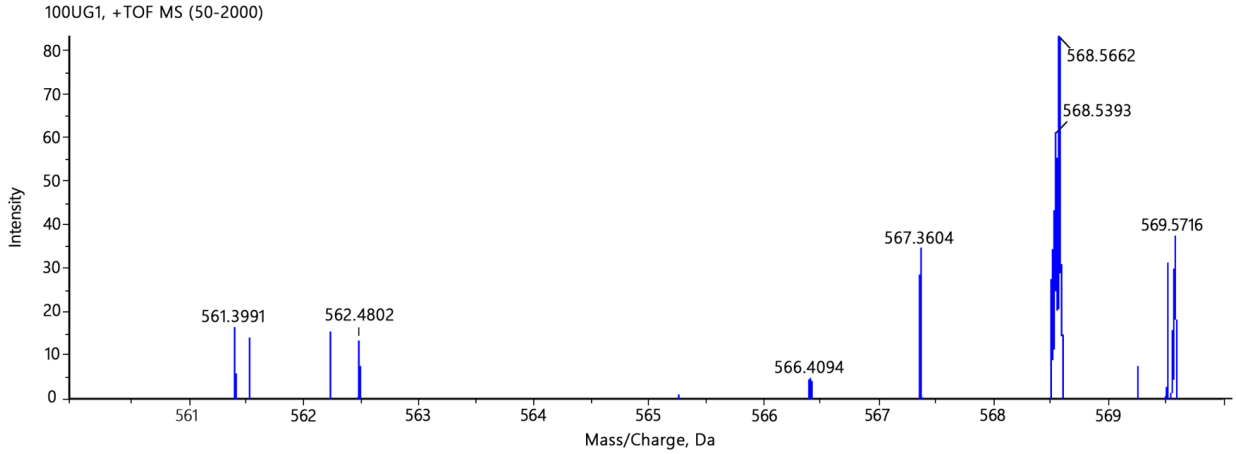

Figure 8. TOF-MS of the Fe-loaded organic phase.

Based on the aforementioned research findings, the primary extracted complex in the Fe-loaded organic phase was $R_4N{\cdot}FeCl_4$. Therefore, the extraction mechanism of Fe was an anion exchange process in the HLNW. Under high-HCl-concentration conditions, Fe^{3+} cation coordinated with Cl^- to form the $FeCl_4^-$ anion. The $FeCl_4^-$ anion then underwent an anion exchange with the Cl^- ions of Aliquat 336, resulting in the formation of $R_4N{\cdot}FeCl_4$. The reaction equation is as follows:

$$Fe^0 + 3HCl = FeCl_3 + 1.5H_2 \quad (6)$$

$$FeCl_3 + HCl = FeCl_4^- + H^+ \quad (7)$$

$$[R_4N \cdot Cl] + FeCl_4^- = [R_4N \cdot FeCl_4] + Cl^- \quad (8)$$

However, in the hydrochloric acid solution of NdFeB waste, REEs were not coordinated with Cl^-, and thus remained as REE^{3+} cations. Consequently, they could not undergo a chemical reaction with Aliquat 336 in the form of anion exchange. Therefore, the selective extraction and separation mechanism for Fe and REEs in the HLNW was as follows: Fe was selectively extracted into the organic phase in the form of $FeCl_4^-$ anions by Aliquat 336, while REEs remained in the aqueous phase as cations, thereby achieving effective separation of Fe and REEs.

3.1.7. Recovery of REEs from the Raffinate

As shown in Table 2, the REEs concentration in the raffinate was 33 g/L, while the iron concentration was only 0.006 g/L. Therefore, recovering REEs from the raffinate is feasible. Oxalic acid precipitation is a widely used method for REEs recovery. Based on our previous research [20], solid oxalic acid was added to the raffinate at a molar ratio of 4.5:1 (oxalic acid to rare earth). The reaction was carried out at 60 °C for 30 min, followed by filtration, washing, and drying to obtain a white precipitate. Under these conditions, 98.36% of the REEs were precipitated. XRD and SEM analyses of the precipitate are presented in Figure 9. The results confirmed that the product was rare earth oxalate hydrate, $RE_2(C_2O_4)_3{\cdot}10H_2O$,

with a granular and flaky morphology. Chemical composition analysis, as detailed in Table 4, indicates that the purity of the recovered rare earth oxalate reached 99.25%.

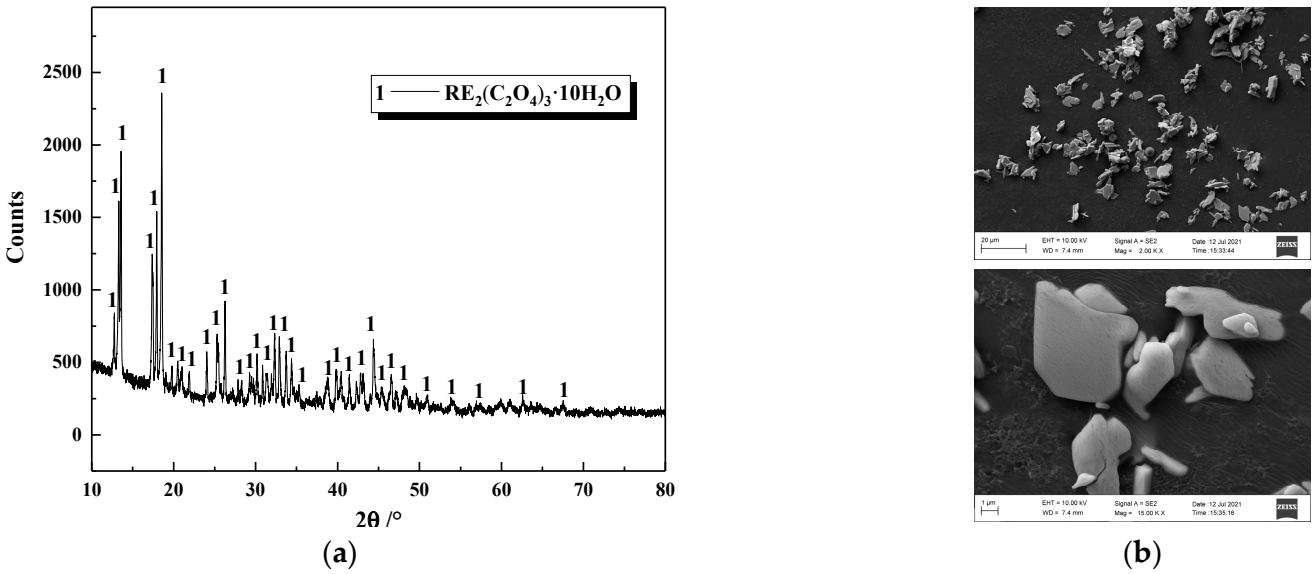

Figure 9. XRD (**a**) and SEM (**b**) of the white precipitate.

Table 4. Chemical composition of $RE_2(C_2O_4)_3 \cdot 10H_2O$ (wt %).

REEs	Fe	Si	Ca	Al
39.53	0.068	0.005	0.07	0.005

3.2. Stripping and Recovery of Fe

3.2.1. Effect of NaOH Concentration on the Fe Stripping

NaOH is a widely used stripping agent in various processes. Upon reacting with the Fe-loaded organic phase, OH^- ions from NaOH exchange with $FeCl_4^-$ ions in the extracted complex, facilitating the release of Fe into the aqueous phase and thereby achieving efficient Fe stripping. This study investigates the influence of varying NaOH concentrations on the stripping efficiency of Fe from the Fe-loaded organic phase. Experiments were conducted at a fixed phase ratio of O/A = 2:1 and a stripping duration of 2 min. The results are presented in Figure 10.

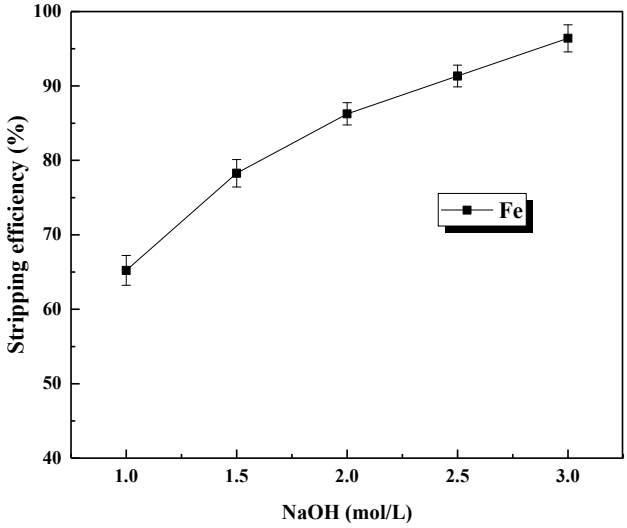

Figure 10. Effect of NaOH concentration.

As shown in Figure 10, the Fe stripping efficiency progressively increased with rising NaOH concentration. At a NaOH concentration of 1 mol/L, the iron stripping efficiency was relatively low at 65.21%. When the NaOH concentration was increased to 2 mol/L, the Fe stripping efficiency reached 86.25%. Further elevating the NaOH concentration resulted in only marginal improvements in stripping efficiency while significantly impacting phase separation due to excessively high alkalinity. Therefore, an optimal NaOH concentration of 2.0 mol/L was selected for the stripping agent.

3.2.2. Effect of Phase Ratio on the Fe Stripping

The effect of the stripping phase ratio (O/A) on the Fe stripping efficiency was investigated using NaOH as the stripping agent. The NaOH concentration was maintained at 2.0 mol/L, and the stripping duration was set to 2 min. The experimental findings are presented in Figure 11.

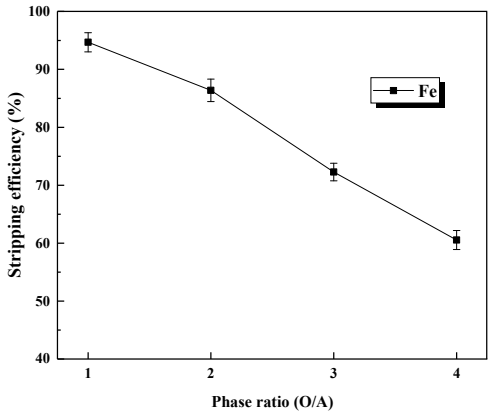

Figure 11. Effect of phase ratio.

As illustrated in Figure 11, the Fe stripping efficiency progressively decreased as the phase ratio O/A increased. At a phase ratio of 1:1, the Fe stripping efficiency was relatively high at 94.68%, although iron was not effectively enriched in the aqueous phase. When the O/A ratio increased to 2:1, the Fe stripping efficiency decreased to 86.38%. Further increasing the O/A ratio resulted in a more substantial decline in the stripping efficiency. Therefore, an optimal phase ratio of O/A = 2:1 was selected for the stripping process.

3.2.3. Countercurrent Stripping of Fe

Based on the optimal conditions, a three-stage countercurrent stripping was conducted. The NaOH concentration was set at 2.0 mol/L, the phase ratio O/A was maintained at 2:1, and the stripping duration was 2 min. The experimental results are presented in Table 5. The findings demonstrated that after three-stage countercurrent stripping, the Fe stripping efficiency reached 99.21%, indicating near-complete recovery of Fe into the aqueous phase by the NaOH solution. The Fe content in the barren organic phase remained minimal, confirming the excellent stripping performance of NaOH for Fe-loaded organic phases.

Table 5. Results of the three-stage countercurrent stripping.

	Fe Concentration (g/L)	Fe Stripping Efficiency (%)
Fe-loaded organic phase	15.17	
Barren organic phase	0.12	99.21
Fe-rich solution	30.10	

Given that the complex in the organic phase was $R_4N{\cdot}FeCl_4$, the mechanism of Fe stripping followed an anion exchange process. Specifically, OH^- ions exchanged with

$FeCl_4^-$ ions at a molar ratio of 1:1, enabling $FeCl_4^-$ to re-enter the aqueous phase. Subsequently, $FeCl_4^-$ reacted with OH^- ions in the aqueous phase at a molar ratio of 1:3 to form $Fe(OH)_3$ colloid, thereby facilitating the Fe stripping. The reaction equations of the stripping are as follows:

$$[R_4N \cdot FeCl_4] + OH^- = [R_4N \cdot OH] + FeCl_4^- \quad (9)$$

$$FeCl_4^- + 3OH^- = Fe(OH)_3 \downarrow + 4Cl^- \quad (10)$$

3.2.4. Recovery of Fe from the Fe-Rich Solution

The red-brown $Fe(OH)_3$ colloid generated during the stripping process was characterized by XRD and FTIR, and the results are shown in Figure 12. The result in Figure 12a indicates that the characteristic peaks of the red-brown precipitate were diffuse peaks, suggesting that the precipitate was amorphous. The result in Figure 12b shows that the characteristic peaks at 3410 cm^{-1} and 1623 cm^{-1} were attributed to ν(O—H) and ν(H—O—H) functional groups, respectively [25,26], and the peak at 1097 cm^{-1} belonged to ν(Fe—OH), while the peaks at 552 cm^{-1} and 473 cm^{-1} were both ν(Fe—O) functional groups [27]. Therefore, it could be further confirmed that the red-brown precipitate was $Fe(OH)_3$. The purity of $Fe(OH)_3$ was analyzed. The results in Table 6 show that the Fe content of this $Fe(OH)_3$ is 51.88%, with a low impurity content. Through theoretical calculation, its purity was 99.16%. The $Fe(OH)_3$ precipitate can be readily recovered by centrifugation or filtration and thermally treated to yield α-Fe_2O_3, a stable, value-added material that can be used in catalysis, pigments, or magnetic storage. Its composition and morphology—dictated by extraction conditions—may further enable direct use in environmental remediation or as a precursor for iron-based nanomaterials.

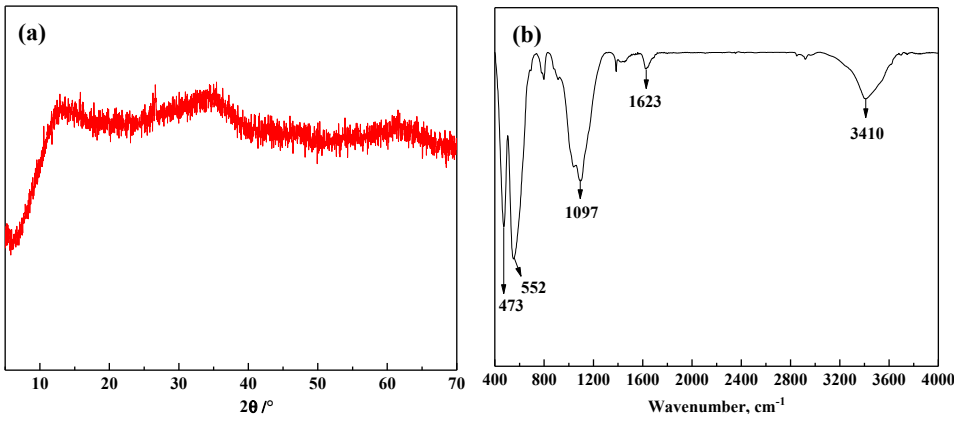

Figure 12. Characterization results of the reddish-brown precipitate. (**a**) XRD and (**b**) FTIR.

Table 6. Chemical composition of $Fe(OH)_3$ (%).

Items	Fe	REEs	Si	Ca	Al
Content	51.88	0.09	0.009	0.01	0.007

3.3. Regeneration and Recycling of the Organic Phase

To regenerate the organic phase, the barren organic phase was treated with hydrochloric acid under optimized conditions. Specifically, a hydrochloric acid concentration of 1.5 mol/L, a phase ratio of 1:1, and a reaction time of 5 min were employed. This process was repeated three times to achieve the regeneration of the organic phase.

To evaluate the extraction efficiency, Fe was extracted from a fresh HLNW using the regenerated organic phase. Subsequently, Fe was stripped from the Fe-loaded organic

phase, and the regeneration process was repeated multiple times in a cyclic manner. The Fe extraction efficiencies were recorded at the end of each cycle to assess the performance of the regenerated organic phase. The results of this regeneration study are summarized in Table 7.

Table 7. Extraction performance of the regenerated organic phase.

Number of regenerations	0	1	2	3	4	5
Extraction efficiency of Fe (%)	99.92	99.86	99.77	99.84	99.70	98.68

The results presented in Table 4 demonstrate that the regenerated organic phase maintained a high extraction efficiency even after five cycles. This indicates that the regenerated organic phase exhibited a robust extraction performance despite repeated regeneration. Due to the alkaline nature of quaternary ammonium bases, the regeneration of the barren organic phase can be accomplished through washing with hydrochloric acid. The reaction equation is as follows:

$$[R_4N \cdot OH] + HCl = [R_4N \cdot Cl] + H_2O \quad (11)$$

3.4. Flowsheet of Separation and Recovery of Fe and REEs

Based on the investigation and analysis, a process flowchart for the separation and recovery of Fe and REEs from HLNW via solvent extraction using Aliquat 336 is proposed in Figure 13. Under optimal conditions, 99.92% of Fe and only 0.18% of REEs were extracted. Subsequently, 98.36% of the REEs were precipitated as $RE_2(C_2O_4)_3 \cdot 10H_2O$, achieving a purity of 99.25%. Furthermore, 99.21% of Fe was stripped using a NaOH solution, followed by precipitation of 98.73% of Fe as $Fe(OH)_3$ with a purity of 99.16%. Finally, the barren organic phase was regenerated with HCl and reused in the extraction cycle. This process enabled the recovery of 98.18% of REEs and 97.87% of Fe from HLNW. The proposed approach demonstrates significant advantages, including high resource utilization efficiency and a simplified, integrated workflow.

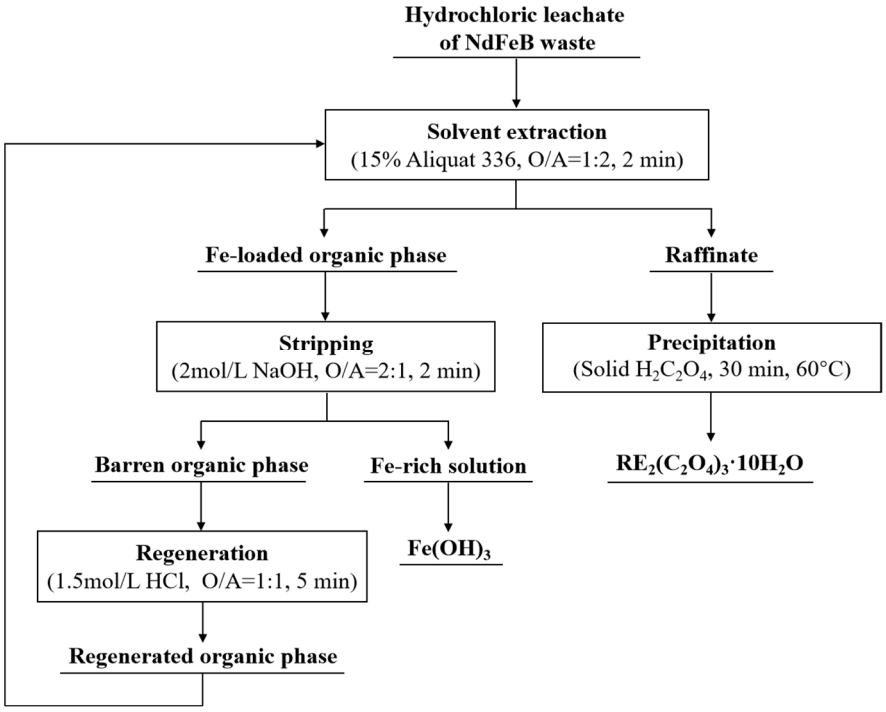

Figure 13. Process flowchart for the separation and recovery of Fe and REEs from HLNW.

4. Conclusions

(1) A novel process for the separation and recovery of Fe and REEs from HLNW via solvent extraction using Aliquat 336 has been developed. This process achieved a recovery efficiency of 98.18% for REEs, with a product purity of 99.25% as $RE_2(C_2O_4)_3 \cdot 10H_2O$, and 97.87% for Fe, with a product purity of 99.16% as $Fe(OH)_3$. Compared to conventional solvent extraction methods for REEs, this approach not only enabled efficient separation and recovery of both Fe and REEs but also offers significant advantages, including high resource utilization efficiency and a simplified, integrated workflow.

(2) Under the conditions of 15% Aliquat 336 concentration, an organic-to-aqueous phase ratio (O/A) of 1:2, and an extraction time of 2 min, HLNW was subjected to three-stage countercurrent extraction, achieving a Fe extraction efficiency of 99.92% and a REEs extraction efficiency of only 0.18%, with a separation factor of 695,200 between Fe and REEs. The extraction and separation mechanisms of Fe and REEs were elucidated using FTIR, UV-vis, and TOF-MS. In the HLNW, Fe existed as $FeCl_4^-$ anions, whereas REEs existed as REE^{3+} cations. The extraction of Fe proceeded via an anion exchange mechanism. Fe was selectively extracted into the organic phase in the form of $FeCl_4^-$ anions by Aliquat 336, while REEs remained in the aqueous phase as cations, enabling effective separation of Fe and REEs.

Author Contributions: Methodology, Z.L., Q.L. and E.L.; Software, L.Y. and Q.L.; Formal analysis, L.Y., Z.Z., Q.L. and H.L.; Investigation, L.Y., Z.L., Z.Z., Q.L., E.L. and H.L.; Resources, Z.L., Z.Z. and H.L.; Data curation, Z.L., Z.Z., E.L. and H.L.; Writing—original draft, L.Y.; Writing—review & editing, Z.L.; Project administration, Z.L.; Funding acquisition, Z.L. All authors have read and agreed to the published version of the manuscript.

Funding: This study was financially supported by the Natural Science Foundation of Jiangxi Province (No. 20242BAB25242), Open fund of Key Laboratory for Ferrous Metallurgy and Resources Utilization of Ministry of Education (NO. NPISlab25-02), and Innovation and Entrepreneurship Training Program for College Students at Higher Education Institutions in Jiangxi Province (NO. S202410407071 and S202410407073).

Data Availability Statement: The original contributions presented in this study are included in the article. Further inquiries can be directed to the corresponding author.

Conflicts of Interest: The authors declare no conflict of interest.

References

1. Wu, J.; Wang, D.; Zhang, Z.; Ye, C.; Wang, Z.; Hu, X. Mechanical activation induced treatment for the synergistic recovery of valuable elements from spent NdFeB magnets. *Waste Manag.* **2024**, *178*, 76–84. [CrossRef]
2. Zheng, H.; Ding, Y.; You, S.; Ding, Y.; Zhang, S.; Zhang, J. A comprehensive review of neodymium-iron-boron (NdFeB) waste recycling: Processes, mechanisms, and prospects. *J. Environ. Manag.* **2025**, *391*, 126513. [CrossRef] [PubMed]
3. Xu, X.; Jia, X.; Zhao, K.; Xu, P.; Jing, P.; Liu, B.; Zhang, J. Recent progress in electrochemical recycling of waste NdFeB magnets. *Chem. Commun.* **2025**, *61*, 2257–2268. [CrossRef] [PubMed]
4. Jyothi, R.K.; Thenepalli, T.; Ahn, J.W.; Parhi, P.K.; Chung, K.W.; Lee, J.-Y. Review of rare earth elements recovery from secondary resources for clean energy technologies: Grand opportunities to create wealth from waste. *J. Clean. Prod.* **2020**, *267*, 122048. [CrossRef]
5. Kumari, A.; Sinha, M.K.; Pramanik, S.; Sahu, S.K. Recovery of rare earths from spent NdFeB magnets of wind turbine: Leaching and kinetic aspects. *Waste Manag.* **2018**, *75*, 486–498. [CrossRef]
6. Xin, W.; Deng, Y.; Jiang, Y.; Zhang, J.; Chen, D. Sulfurization Roasting Process of Nd_2O_3 and Synthetic $NdFeO_3$ with Ferric Sulfate. *Metall. Mater. Trans. B* **2021**, *52*, 2151–2162. [CrossRef]
7. Önal, M.A.R.; Aktan, E.; Borra, C.R.; Blanpain, B.; Van Gerven, T.; Guo, M. Recycling of NdFeB magnets using nitration, calcination and water leaching for REE recovery. *Hydrometallurgy* **2017**, *167*, 115–123. [CrossRef]
8. Zhang, Z.; Wang, D.; Liu, C.; Zhi, W.; Xiao, W.; Qian, G.; Li, G. New insight into oxidative roasting and leaching for NdFeB waste. *J. Environ. Chem. Eng.* **2022**, *10*, 108946. [CrossRef]

9. Chen, L.; Li, H.; Chen, J.; Li, D.; Liu, T. Separation of heavy rare earths by di-(2-ethylhexyl) phosphinic acid: From fundamentals to cascade extraction simulation. *Miner. Eng.* **2020**, *149*, 106232. [CrossRef]
10. Fu, Y.; Huang, M.; Zhou, Z.; Li, Z.; Liao, W.; Lu, Y. Separation of trivalent rare earths from nitrate medium using solvent extraction with a novel extractant 2-ethylhexyl ((2-ethylhexylamino)methyl) phosphonic acid. *J. Rare Earths* **2022**, *40*, 491–500. [CrossRef]
11. Liu, Q.; Tu, T.; Guo, H.; Cheng, H.; Wang, X. High-efficiency simultaneous extraction of rare earth elements and iron from NdFeB waste by oxalic acid leaching. *J. Rare Earths* **2020**, *39*, 323–330. [CrossRef]
12. Nayl, A.A. Extraction and separation of Co(II) and Ni(II) from acidic sulfate solutions using Aliquat 336. *J. Hazard. Mater.* **2010**, *173*, 223–230. [CrossRef] [PubMed]
13. Liu, Z.; Huang, J.; Zhang, Y.; Liu, T.; Hu, P.; Liu, H.; Luo, D. Separation and recovery of vanadium and aluminum from oxalic acid leachate of shale by solvent extraction with Aliquat 336. *Sep. Purif. Technol.* **2020**, *249*, 116867. [CrossRef]
14. Xu, Z.-G.; Zhou, T.; Zou, Q.; Yang, F.; Wang, Y.-X.; Wang, S.-C.; Wang, C.-H. Solvent extraction of Ni and Co from Ni-laterite leach solutions using a new synergistic system consisting of Versatic 10 acid, Mextral 6103H and Aliquat 336 with elemental mass balance for leaching, precipitation, solvent extraction, scrubbing and stripping. *Hydrometallurgy* **2022**, *208*, 105822. [CrossRef]
15. Ahmed, A.G.; Basma, T.M.; Shaimaa, S.A.; Said, I.M.; Nagwa, I. Solvent extraction of titanium (IV) from orthophosphoric acid media using Aliquat-336/kerosene and stripping with nitric acid. *Hydrometallurgy* **2025**, *231*, 106403.
16. Liu, Z.; Huang, J.; Zhang, Y.; Liu, T.; Hu, P.; Liu, H.; Zheng, Q. Separation and recovery of vanadium and iron from oxalic-acid-based shale leachate by coextraction and stepwise stripping. *Sep. Purif. Technol.* **2020**, *244*, 116532. [CrossRef]
17. Li, J.-T.; Gao, L.-L.; Zhao, Z.-W.; Liu, X.-H.; Chen, X.-Y. Efficient recovery of tungsten from scheelite concentrates using a sulfur-phosphorus mixed acid leaching system. *Tungsten* **2024**, *6*, 821–832. [CrossRef]
18. Cui, L.; Cheng, F.; Zhou, J. Preparation of high purity $AlCl_3{\cdot}6H_2O$ crystals from coal mining waste based on iron(III) removal using undiluted ionic liquids. *Sep. Purif. Technol.* **2016**, *167*, 45–54. [CrossRef]
19. Sahar, B.; Simon, C.; Fabrice, G.; Stéphane, P.; Alain, S.; Nourredine, M.; Guilhem, A. Selective recovery of rare earth elements from acetic leachate of NdFeB magnet by solvent extraction. *Sep. Purif. Technol.* **2024**, *339*, 126701.
20. Liu, Z.; Zhou, H.; Li, W.; Luo, X.; Wang, J.; Liu, F. Coextraction of Fe and REEs from NdFeB sludge by co-leaching and stepwise precipitation. *Sep. Purif. Technol.* **2022**, *282*, 119795. [CrossRef]
21. Liu, Z.; Huang, J.; Zhang, Y.; Liu, T.; Hu, P.; Liu, H.; Zheng, Q. Separation and Recovery of Iron Impurities from a Complex Oxalic Acid Solution Containing Vanadium by $K_3Fe(C_2O_4)_3{\cdot}3H_2O$ Crystallization. *Sep. Purif. Technol.* **2020**, *232*, 115970. [CrossRef]
22. Fujita, J.; Martell, A.E.; Nakamoto, K. Infrared Spectra of Metal Chelate Compounds. VI. A Normal Coordinate Treatment of Oxalato Metal Complexes. *J. Chem. Phys.* **1962**, *36*, 324–331. [CrossRef]
23. Bal, Y.; Bal, K.E.; Cote, G.; Lallam, A. Characterization of the solid third phases that precipitate from the organic solutions of Aliquat® 336 after extraction of molybdenum(VI) and vanadium(V). *Hydrometallurgy* **2004**, *75*, 123–134. [CrossRef]
24. Cui, L.; Cheng, F.; Zhou, J. Behaviors and mechanism of iron extraction from chloride solutions using undiluted Cyphos IL 101. *Ind. Eng. Chem. Res.* **2015**, *54*, 7534–7542. [CrossRef]
25. Saritha, A.; Raju, B.; Hussain, K.A. Synthesis and Characterization of 3D Chiral Anhydrous Potassium Tris(oxalato)Ferrate(III): A Way Towards Multifunctional Applications. *J. Comput. Theor. Nanosci.* **2013**, *19*, 885–888. [CrossRef]
26. Abhishek, L. Influence of Ascorbate and Oxalic Acid for the Removal of Iron and Alkali from Alkali Roasted Ilmenite to Produce Synthetic Rutile. *Ind. Eng. Chem. Res.* **2010**, *49*, 8847–8851. [CrossRef]
27. Wang, H.-L.; Cui, J.-Y.; Jiang, W.-F. Synthesis, characterization and flocculation activity of novel $Fe(OH)_3$—Polyacrylamide hybrid polymer. *Mater. Chem. Phys.* **2011**, *130*, 993–999. [CrossRef]